THE JOURNAL OF PHYSICAL CHEMISTRY B

Article

Octaoctyl Substituted Lutetium Bisphthalocyanine For NADH Biosensing

Chandana Pal, Ashwani K Sharma, Andrew N. Cammidge, Michael John Cook, and Asim K Ray

J. Phys. Chem. B, **Just Accepted Manuscript** • Publication Date (Web): 08 Nov 2013

The Journal of Physical Chemistry B is published by the American Chemical Society.
1155 Sixteenth Street N.W., Washington, DC 20036

Octaoctyl Substituted Lutetium Bisphthalocyanine for NADH Biosensing

C. Pal[1], A. K. Sharma[2], A. N. Cammidge[3], M. J. Cook[3] and A. K. Ray[1]

[1]The Wolfson Centre for Materials Processing, Brunel University, Uxbridge, Middlesex UB8 3PH, UK

[2]USAF, Research Laboratory, Space Vehicles Directorate, SE Kirtland AFB, NM 87117 USA

[3]School of Chemistry, University of East Anglia, Norwich NR4 7TJ, UK

ABSTRACT

Cyclic voltammetric and Raman and UV-vis spectroscopic measurements were performed on thin films of non-peripherally substituted bis[1,4,8,11,15,18,22,25-octakis(octyl)phthalocyaninato] lutetium(III) ($R_{16}LuPc_2$). Voltammograms exhibit one-electron quasi-reversible redox processes in 1.5M $LiClO_4$ aqueous solutions. The red-shift of the Q-band of $R_{16}LuPc_2$ in the UV-visible absorption spectra upon oxidation is attributed to the shortening of the inter-ring distance between the two phthalocyanine moieties. This observation is also consistent with the shift in the redox-sensitive vibrational modes in the Raman spectra due to the localization of the positive charge on phthalocyanine moieties. Neutralization of the oxidized $R_{16}LuPc_2^+$ film by dihydronicotinamide adenine dinucleotide (NADH) using different concentrations varying from 0.05 mM to 3 mM has been studied by UV-vis absorption and Raman spectroscopies. The reduction processes for a three month old film were found to be slower than those for freshly prepared films and showed a dependence upon NADH concentration. The data provide a basis for application of $R_{16}LuPc_2$ as a sensor for NADH.

Key words: Lanthanide complexes, Oxidation and reduction**,** Formal potential, Isosbestic points, Ion transfer, Raman spectroscopy.

1. Introduction

Lanthanide bisphthalocyanines are sandwich complexes in which a lanthanide ion is bound to two phthalocyanine (Pc) rings. All the lanthanides other than cerium are found only in the trivalent state and thus their binding to two Pc^{2-} ligands leads to interesting redox properties.[1] The compounds have been extensively used in a variety of sensing applications in environmental monitoring, food quality control and health care.[2-5] Their intrinsic semiconductivities are higher than those of monophthalocyanine analogues enabling high sensitivity resistive sensors to be developed for monitoring pollutant gases and volatile organic compounds.[6] Due to an intramolecular charge transfer, optical absorption spectra display an intense band corresponding to the incident wavelengths in the telecommunication-compatible near-infrared region between 1400 nm and 1600 nm. The disappearance of this band upon the addition of oxidant or reducing gases has led to the fabrication of fibre optic sensors to detect volatile organic compounds such as acetic acid, ethanol, n-butyl acetate and hexanal that contribute to the aroma of wines at different concentrations over a range from 4 mM to 88 mM.[7] The electrochromic properties of lanthanide bisphthalocyanines involving one-electron oxidation and reduction processes of the phthalocyanine rings is very specific to the type of the electrolytic solution used. The development of electronic noses and tongues has thus been proposed based on highly sensitive, reproducible voltammetric measurements for phenolic acids such as vanillic and ferlulic (monophenol), catechol and caffeic (diphenols), and gallic and pyrogallol (triphenols) to the limit of 10^{-6}M .[8,9] These studies are important for the quality control, classification, freshness evaluation and authenticity assessment of a variety of food, mainly wines and olive oils.

The realisation of reduced nicotinamide adenine dinucleotide (NADH) biosensing probes is currently attracting considerable attention for monitoring mitochondrial function as an electron exchanger.[10,11] Electron transfer takes place through the oxidation of NADH with the regeneration of the corresponding oxidized form (NAD^+) producing sufficient adenosine triphosphate enzymes for cellular energy supply to sustain normal brain functions. Oxyradicals which are also produced from NAD^+ to NADH redox reactions are detrimental to brain proteins, causing age-related diseases like Alzheimer's and Parkinson's diseases.[12] NADH sensors have also been identified for possible use for determining the training efficiency of athletes, diagnosis of cortical spreading depression and monitoring jet-lag induced fatigue.[13-15] This intense interest has led to the development of electrochemical sensors employing a host of carbon based nanomaterials including graphene.[16-18]

We have studied in recent years the effect of NADH reduction on optical absorption spectra of oxidised films of solution processable substituted lanthanide bisphthalocyanine complexes metallated with dysprosium and lutetium.[19-21] The spin coated films deposited on glass substrates were chemically oxidized either by saturated bromine vapour or concentrated nitric acid vapours. The phthalocyanine Q-

band is red shifted upon oxidation of the complexes. The process of NADH reduction of the oxidised complexes to the original neutral state is found to be governed by first-order kinetics. The functionalized layer shows an efficient activity towards the NADH at concentration as low as 1×10^{-5} M.

This article develops these findings further in terms of Raman spectroscopic investigations and reports the results of cyclic voltammetric studies to examine electroactive species of spin coated films of bis[1,4,8,11,15,18,22,25-octakis(octyl)phthalocyaninato] lutetium(III), Figure 1, and referred to hereafter as $R_{16}LuPc_2$. The symmetrically substituted bisphthalocyanine is readily soluble in common organic solvents, and the substitution of octyl chains promotes self-assembly of the solution processed films. Lutetium is commonly seen as the archetypal lanthanide element and has been incorporated as the lanthanide ion in bis-phthalocyanine complexes both in the present work and by other authors. We have earlier explored the application of the present example of a ring substituted compound for the fabrication of organic field effect transistor [22] and its availability to us is a significant reason for its use in the present work. Raman spectroscopic measurements have been performed to determine the change in electronic distribution within macrocylic rings due to oxidation and reduction. Further investigations are also carried out to determine the active life of the NADH sensing membrane with a view to developing biodevices for the point of care uses.

2. Experimental

The method consists of thin film formulation of $R_{16}LuPc_2$.molecules on suitable substrates for the cyclic voltammetric, Raman and UV-vis absorption spectroscopic measurements with a view to examining the redox interaction between the film and NADH.

2.1 Materials and sample preparation

$R_{16}LuPc_2$ compounds were used as synthesised following our reported synthesis. [22] β-Nicotinamide adenine dinucleotide, reduced disodium salt (NADH of purity approx. 98%), lithium perchlorate ($LiClO_4$; purity approx. 95%) and bromine of reagent grade were procured from Sigma-Aldrich. Solutions of these reagents were prepared in distilled water with resistivity of 18.2 MΩcm to desired concentrations.

Using a spreading solution of $R_{16}LuPc_2$ in chloroform ($CHCl_3$) of concentration 10 mg/ml, a KW-4A spin-coater (Chemat Technology Inc.) was employed at 1000 rpm for 30s to deposit approximately 100nm thick films on ultrasonically cleaned substrates for electrochemical and optical absorption studies. Tetrabutylammonium perchlorate (TBAP) and dichloromethane (DCM) of electrochemical grade, was procured from Sigma Aldrich. 0.1M of TBAP was used as electrolyte for cyclic voltammetry of 0.01 mg/ml $R_{16}LuPc_2$ in DCM solution. Drop cast films were used for Raman measurements. For

redox interaction studies, the as-deposited neutral film was oxidised by exposure to bromine vapour for two minutes. The oxidised films were reduced to neutral by NADH freshly dissolved in an aqueous solution of 1.5M $LiClO_4$.

2.2 Cyclic voltametry

For $R_{16}LuPc_2$ cyclic voltammetric measurements on the $R_{16}LuPc_2$ molecules in the solution, the Ag/AgCl reference electrode was enclosed in a Luggin capillary, filled with the DCM/TBAP mixture. The capillary tip was placed close to the platinum working electrode with a view to minimising the undesirable electrical resistance. The platinum wire counter electrode remained immersed in the DCM/TBAP solution. The voltage was swept between ±2.5 V at 100 mV/sec scan rate. Redox reaction activities were also examined on homogeneous thin films of $R_{16}LuPc_2$ deposited on indium-tin-oxide (ITO) coated glass substrates as a working electrode of a three-electrode GiIIAC potentiostat. A high purity platinum wire counter electrode and an Ag/AgCl reference electrode were used in a three-electrode configuration with a working electrode. The steady state cyclic voltammogram curves were recorded at room temperature in an aqueous medium of 1.5M $LiClO_4$ (pH = 7.2) by potentiodynamic sweep between 0V and 1.5V with a rate of 100mV/sec with respect to the reference electrode. An oxygen free environment was maintained by the constant flow of pure N_2 gas during the voltammetric experiments.

2.3 Spectroscopic measurements

Raman spectra of a drop cast film of $R_{16}LuPc_2$ were recorded using a LabRam Raman spectrometer (Horiba Jobin Yvon) equipped with an 1800 groove mm^{-1} holographic grating, a holographic super-notch filter (Kaiser), an Olympus BX40 microscope and a Peltier-cooled CCD (MPP1 chip) detector. A He–Ne laser provided the excitation radiation at 632.8 nm; the laser beam was attenuated by a 10% neutral density filter, resulting in a laser power of 0.8 mW at the sample. Backscattering geometry was used in all experiments. All Raman measurements involved acquisition of multiple spectral windows in the range 200-1700cm^{-1} (Stokes shifts only). The Raman spectra of solid samples on a microscopic glass slide were collected at room temperature using a microscope objective of ×100 magnification to focus the laser beam.

Spin coated films of oxidised films of $R_{16}LuPc_2$were reduced by NADH freshly dissolved in an aqueous solution of 1.5M $LiClO_4$ in a 1 cm pathlength quartz cuvette. Transient spectral changes arising from chemichromic modification of the $R_{16}LuPc_2$ spun films on treatment with 3mM of NADH were recorded *in situ* using a UV-Vis spectrophotometer (Perkin Elmer LAMBDA 650) in the range 400 to

850 nm using a 654.92 nm/min scan rate. Addition of $LiClO_4$ was used to control the rate of reduction of the oxidised $R_{16}LuPc_2$ film.

3. Results and discussions

3.1 Cyclic-Voltammetry

Figure 1(b) shows a typically reproducible cyclic voltammogram of the $R_{16}LuPc_2$ molecules in the solution phase, displaying the presence of two anodic potential peaks E_{pa} at +1.54V and -0.40V and two cathodic potential peaks at +0.365mV and -1.26V in the voltage sweep between ±2.5V. These lead to the formation of monovalent cations and anions respectively and can be represented in the form:

$$R_{16}LuPc_2^- \underset{+e-}{\overset{-e-}{\rightleftharpoons}} R_{16}LuPc_2 \underset{+e}{\overset{-e-}{\rightleftharpoons}} R_{16}LuPc_2^+$$

Values of the formal potential (E_0) and the peak potential separation ΔE for are estimated to be 0.95V and 1.175V for oxidation from the knowledge that $E_0 = (E_{pa} + E_{pc})/2$ and $\Delta E = (E_{pa} - E_{pc})$. Using the same relations, E_0 = -0.81V and ΔE = 0.86V were obtained for reduction process. The difference between the formal potentials for oxidation and reduction is found to be 1.76V. This value corresponds well to the HOMO–LUMO gap of the molecule.[23]

A single pair of the peak anodic cathodic potentials was observed in the voltammogram in Figure 1(c) for spin coated films of $R_{16}LuPc_2$ molecules for voltage sweep between 0V and 1.5V. As the voltage was increased from 0V to1.5V, the film became progressively oxidised, displaying the anodic peak currents (i_{pa}) of 0.046 $mAcm^{-2}$ at the peak anodic potential E_{pa} = 0.70V vs the reference electrode. The cathodic (i_{pc}) peak current of 0.12 $mAcm^{-2}$ was observed at the cathodic potential E_{pc} = 0.41 V, giving rise to the reduction of the film in the reverse sweep. Values of the formal potential (E_0) and the peak potential separation ΔE are estimated to be 0.56V and 0.29V.

The characteristic value of ΔE = 59mV for one electron reversible process is much smaller than those obtained for the $R_{16}LuPc_2$ molecules in both solution and solid phases. The large values of ΔE may be attributed to due to the effect of substitution of octyl ($-C_8H_{17}$) chains at non-peripherial positions of the $R_{16}LuPc_2$ molecules.[24] This observation is also supported by the earlier work on similarly non-peripherally substituted octa-alkylated metal-free phthalocyanine molecules.[25] Values of ΔE became greater with increasing length of substituted alkyl chains length leading to the diminished degree of reversibility. The effect of the substitution on the formal potential E_0 is also reported. For example, E_0 = 0.78V was observed for the drop cast film of the double-decker lutetium(III) phthalocyanine molecules, substituted with dodecyl ($-C_{12}H_{25}$) on each ring.[26]

The ratio of the anodic (i_{pa}) to cathodic (i_{pc}) peak currents is estimated to be 0.35, implying that only about one third of neutral $R_{16}LuPc_2$ on the forward sweep become reoxidised to $R_{16}LuPc_2^+$ on the reverse sweep. The electron transfer is, therefore, a quasi-reversible process which is not completely in electrochemical nature but is expected to have involved other physical or chemical processes. Values of $2.20\times10^{-3}cms^{-1}$, 1.0×10^{-5} $cm^2s^{-1}$and 0.5 were deduced for the heterogeneous electron transfer rate constant, diffusion coefficient and charge transfer coefficient respectively from the numerical solution of the Tafel equation for the forward sweep.[27]

As the overall reaction equilibrium depends upon the ion transfer energetics, the choice of the electrolytes is important for an observable electron transfer in the polarization domain.[28] Cyclic voltammetric measurements were repeated using 1 M aqueous KCl (pH = 7.0) as electrolyte in order to determine the electrolyte dependent stability of the working electrode. Ion exchange reactions between the electrolyte ions and the ions in the aqueous phase can alter the starting conditions for the electron transfer reaction.[29] As shown in the inset, the anodic peak current i_{pa} decreased with the number of cycles up to 10 cycles. Similar instability was also observed in voltammograms of an electrophoretically deposited film of a different lutetium bisphthalocyanine derivative.[30] It shows that the KCl electrolyte counter anions became less active in forming the counterion on the singly oxidized form of $R_{16}LuPc_2^+$ possibly due to penetration of KCl into the film. This ion-pairing effect caused the degradation of anodic peak current i_{pa} with the voltage cycling. However, the peak current remained largely stable for the 1.5 M $LiClO_4$ electrolyte solution indicating invariant nature of ion-paring with supporting electrolyte anions.[31]

The current-time transient curves were recorded under the application of a constant oxidising potential of 0.88V. As shown in Figure 1(d), a sharp spike to current density of $11\mu A/cm^2$ was observed at the start. The plot in the inset of the current density against the time on logarithmic scales is linear over the time less than 60sec, giving a value of 0.53 for the slope. This implies the validity of the Cottrell law.[32] The oxidation of the $R_{16}LuPc_2$ thin film was found to be complete within the period of 60sec, which is due to the accumulation ClO_4^- near the working electrode. After this time, the rate of diffusion of the ions to the interface between the $R_{16}LuPc_2$ film and the electrolyte was much slower than that of the oxidation process, giving rise to the rapid drop of current.

3.2 Optical absorption spectroscopy

Figure 2 presents the optical absorption spectra of $R_{16}LuPc_2$ in freshly prepared chloroform solution and films, both as neutral and oxidised states. Both Valence effective and extended Huckel Hamiltonian calculations have shown that the characteristic features primarily depend upon the phthalocyanine ring separation distance and the stagger angle between the two macrocyclic rings.[33,34] In the case of $R_{16}LuPc_2$

it is found to be 39.1º from a single crystal X-Ray crystallographic study. The static symmetry of the molecule is, therefore, considered to be D4($P2_1/a$).[35] As shown in the inset, the split Q-band at 714 nm and 634 nm and the radical band at 473 nm in the absorption spectrum of $R_{16}LuPc_2$ in chloroform solution may therefore be assigned to the $a_2 \rightarrow e_3$, $b_1 \rightarrow e_1$ and $e_1 \rightarrow a_2$ transitions, respectively.[36] The Q-band position at 714 nm is consistent with the earlier observation the cyclic voltammetry measurements of 1. 1.76V for the difference in the formal potential. The orbitals a_2 and b_1 which are associated with the centre of the ring carbon atoms represent π-π* interactions depending upon the inter-ring distance. The lowest unoccupied e_1 and e_3 orbitals are centred on the pyrrole and isoindole nitrogens. The positions of the split Q-band in the neutral film spectrum on the ITO glass substrate are found to be at 718nm and 652nm, respectively. The small red-shift of the Q-band indicates that molecules may develop J-type aggregates in the thin film. The spin coated $R_{16}LuPc_2$ thin film was oxidised in an aqueous medium of 1.5 M $LiClO_4$ by applying a bias potential of 0.88V for 20 minutes. Spectra for both neutral and bromine oxidised films are included for the sake of comparison. Oxidised films display a red shift of the Q-band from 718 nm to 778 nm due to the possible removal of the electrons in the anti-bonding HOMO, as a result of relatively short Pc–Pc inter-ring distance. This result agrees well with the prediction of the density functional model for lanthanide bisphthalocyanines.[37] The disappearance of the 473 nm band on oxidation is caused by one electron transfer to individual radicals. Similar behaviour was observed for a tert-butylcalix[4]arene bridged dimeric lutetium(III) phthalocyanine on platinum electrode.[38]

In order to determine the effect of ageing, the spectra were recorded for $R_{16}LuPc_2$ samples which had been left in air for 3 months. As shown in Figure 3, the solution of $R_{16}LuPc_2$ in chloroform appears not to suffer from any ageing effect with the Q-band peaks at almost the same positions of 714 nm and 634 nm. On the other hand, the two Q-bands of the 3 month old neutral spin coated film spectrum exhibited two different types of wavelength shifts: a small red shift from 718 nm to 736 nm and a blue shift from 653nm to 643 nm. It is possible that some relaxation of the molecular packing distortion occurs over time. When this film was oxidised by exposure to bromine vapour, the main Q band peak of the oxidised film underwent a blue shift to 772 nm from 736 nm. However this is smaller than that exhibited by a fresh film upon oxidation. The bromine oxidised $R_{16}LuPc_2^+$ film remained stable for at least 3 hours, long enough to examine its interaction with freshly prepared biological cofactor NADH in 1.5M $LiClO_4$ aqueous solution. Figure 4 shows the time dependent neutralisation process of an $R_{16}LuPc_2^+$ film on interaction with 0.5mM NADH over 90 minutes. The isosbestic points are well-defined with the monotonic decrease in the absorption intensity at the 772 nm peak and simultaneous increase in the peak intensity of the 718 nm band with time. The lowering of the intensity of the 772 nm peak was found to

be exponential as evident from the linear plot of absorption intensity against time on a logarithmic-linear scale in the inset (A). The reduction rate constant was found to be 1.12×10^{-2} min^{-1} from the slope. Absorption spectra were recorded for the reduction of an $R_{16}LuPc_2^+$ film by 0.5 mM and 1 mM NADH. As shown in inset (B), values of the half-life of the oxidation of $R_{16}LuPc_2^+$ are found to be decreasing with the concentration of NADH. The NADH reduction of the 3 month old film, when Br_2 oxidised, is consistently slower than a similarly oxidised fresh film, giving a percentage change from 94% for 0.05M to 6% for 1mM concentration of NADH. This detection limit is smaller than the reported value of 8 mM NADH detection with different types of modified electrodes for enzyme-based electrocatalytic systems.[39]

3.3 Raman spectroscopy

Figure 5 shows the Raman spectra in the 200-1700 cm^{-1} range for a drop cast $R_{16}LuPc_2$ film in the neutral and oxidised states. The qualitative assignment of the vibrations of $R_{16}LuPc_2$ was carried out on the basis of a comparison with Raman spectra of different bisphthalocyanine derivatives and the results are summarized in Table 1. The excitation at 633nm is close to the Q-band absorptions. The peaks occurring at 1320-1650 cm^{-1} are, therefore, attributed to C=C pyrrole, isoindole ring and aza C=N stretching.[40] These bands are sensitive to the size of the central tervalent lanthanide ion. The most intense band at 1510 cm^{-1} is the marker band for the monoanion radical species attributed to a $\nu_3$porphyrin-like mode containing nearly equal C=C pyrrole and C=N aza.[41] The macrocycle ring breathing is responsible for the 500-840 bands and the 748 cm^{-1} and 777 cm^{-1} bands are related to aromatic bonding. The Lu-N bond stretching vibrations have caused the occurrence of Raman peaks at frequencies in the range from 200 cm^{-1} -500 cm^{-1}.

The Raman modes of double decker lutetium bisphthalocyanine are sensitive to the removal of an electron from their π-π^* conjugation on phthalocyanine rings after one-electron oxidation with resulting shift in the redox-sensitive vibrational modes. The positive charge (hole) becomes localised on the Pc ring.[42] The hole is delocalised throughout the two macrocycles of a neutral $R_{16}LuPc_2$ film. The charge transfer takes place via the metal and from the Pc ring pyrrole C-N bond, forming a charge transfer $R_{16}LuPc_2^+$-Br_2 complex. The adsorbed bromine evaporates off in due course when the film is left in atmosphere. It is evident from Table 1 that there is a general tendency of vibrational modes moving to higher frequencies on oxidation possibly due to the whole confinement. The maximum shift is observed in the frequency region between 1320 cm^{-1} -1650 cm^{-1}. The NADH interaction is believed to reduce the $R_{16}LuPc_2$ film almost completely to the neutral form as judged by the Raman spectra in Figure 5(d) which is similar to those of the film prior to chemical oxidation (Figure 5a). The processes of reduction and oxidation of $[(C_6H_{13}S)_8Pc]_2Lu$ films may, therefore, be considered reversible.

The drop cast film was left in air for 3 months and Raman spectra, Figure 6(a), were recorded for neutral and oxidised films. The peak positions are included in Table 1, showing very small shifts in frequencies through ageing the film over 3 months. Shifts of the positions due to oxidation are similar to those obtained for the freshly prepared film. The histograms in the inset of Figure 6(b) show the changes in relative intensities of two adjacent bands within the ranges of 748cm^{-1} -780cm^{-1} and 1335 cm^{-1} - 1406 cm^{-1}. The interaction between the macrocycles changes due to change of electron density, affecting the relative intensities of the bonds. The pyrrole and isoindole stretching vibrations in the range 1300–1530 cm^{-1} are believed to be strongly affected by change of electronic distribution due to oxidation of the freshly prepared sample. The hole localisation and delocalisation on the phthalocyanine rings due to oxidation are believed to be comparable for both the freshly prepared and 3 months old sample.

4. Concluding Remarks

The quasi-reversible one-electron redox processes in non-perpheral octaoctyl substituted lutetium bisphthalocyanine ($R_{16}LuPc_2$) molecules are believed from the cyclic voltammetry studies to be independent of the lutetium central ion but associated with ring-based processes during oxidation and reduction. The electrochromic behaviour of the film was examined by cyclic voltammetry establishing the value of 0.88V for bias potential for oxidation. A simple optical method for the detection of NADH on a glass substrate modified with spin coated electrochromic $R_{16}LuPc_2$ film has been investigated with the detection limit of 0.5 mM. The observation from UV-visible absorption and vibrational spectroscopic measurements of the complete recovery of the oxidised bispthalocyanine film to its neutral form via NADH reduction leads to the realisation of reusable membranes to be incorporated in practical biosensors for the point care uses. The $R_{16}LuPc_2$ film remains sensitive at least for three months even when left in open space. However the reduction rate is slow but further work is in progress to develop well-designed calibration protocols.

ACKNOWLEDGEMENTS

This work is sponsored by the Air Force Office of Scientific Research, Air Force Material Command, USAF, under grant no. FA8655-13-1-3018. The authors are also grateful to Dr Lesley Hanna of the Wolfson Centre for Materials Processing, Brunel University for fruitful discussions and input.

References

1. Weiss, R.; Fischer, J.; In The porphyrin handbook, K.M. Kadish, K. M. Smith & R. Guilard Eds; Academic Press, San Diego, CA. 2003, vol. 16 pp. 171–246.

2. Valli, L. Phthalocyanine-based Langmuir–Blodgett films as chemical sensors. Adv. *Colloid Interfac*. 2005,116, 13-44.
3. Martin M. G.; Rodriguez-Mendez, M. L.; de Saja, J. A. Films of Lutetium Bisphthalocyanine Nanowires as Electrochemical Sensors. *Langmuir,* 2010, 26 19217-19224.
4. Apetrei, C.; Alessio, P.; Constantino, C. J. L.; de Saja, J. A.; Rodriguez-Mendez, M. L.; Pavinatto, F. J.; Fernandes, E. G. R.; Zucolotto, V.; Oliveira, O. N. Biomimetic biosensor based on lipidic layers containing tyrosinase and lutetium bisphthalocyanine for the detection of antioxidants. *Biosens. Bioelectron.* 2011, 26, 2513-2519.
5. Durmus, M.; Yesilot, S.; Cosut, B.; Gurek, A. G.; Kilic, A.; Ahsen, V. Comparison of Photophysicochemical Properties of Hexaphenoxycyclotriphosphazenyl-Substituted Metal-free, Mono- And Bis-Lutetium Phthalocyanines. *Synth. Met*. 2010**,** 160, 436-444.
6. Rodriguez-Mendez, M. L.; Gay, M; de Saja, J.A. New Insights into Sensors Based on Radical Bisphthalocyanines *J. Porphyr. Phthalocyanines.* 2009**,** 13**,** 1159-1167.
7. Bariain, C., Matias, I. R., Fernandez-Valdivielso, C., Arregui, F. J., Rodriguez-Mendez, M. L., de Saja, J. A. Optical Fiber Sensor Based on Lutetium Bisphthalocyanine for the Detection of Gases using Standard Telecommunication Wavelengths. *Sens. Actuators, B:* 2003, 93, 153-158.
8. Fernandes, E. G. R.; Brazaca, L. C.; Rodriguez-Mendez, M. L.; de Saja, J. A; Zucolotto, V. Immobilization of Lutetium Bisphthalocyanine in Nanostructured Biomimetic Sensors using the LbL Technique for Phenol Detection. *Biosens. Bioelectron*. 2011, 26, 4715-4719.
9. Pavinatto, F. J.; Fernandes, E. G. R.; Alessio, P.; Constantino, C. J. L.; de Saja, J. A.; Zucolotto, V.; Apetrei, C.; Oliveira, O. N. Jr.; Rodriguez-Mendez, M. L. Optimized Architecture for Tyrosinase-Containing Langmuir-Blodgett Films to Detect Pyrogallol. *J. Mater. Chem.* 2011, 21, 4995-5003.
10. Mayevsky, A.; Barbiro-Michaely, E. Shedding light on mitochondrial function by real time monitoring of NADH fluorescence: II: human studies. *J. Clin. Monitor. Comp.* 2013, 27, 125-145
11. Mayevsky, A.; Barbiro-Michaely, E. Shedding Light on Mitochondrial Function by Real Time Monitoring of NADH Fluorescence: I. Basic Methodology and Animal Studies. *J. Clin. Monitor. Comp*. 2013, 27, 1-34
12. Ghosh, D.; LeVault, K. R.; Barnett, A. J.; Brewer, G. J. A Reversible Early Oxidized Redox State That Precedes Macromolecular ROS Damage in Aging Nontransgenic and 3xTg-AD Mouse Neurons. *J. Neurosci.* 2012, 32, 5821-5832.

13. Nadlinger, K.; Westerthaler, W.; Storga-Tomic, D.; Birkmayer, J. G. D. Extracellular metabolisation of NADH by blood cells correlates with intracellular ATP levels. *Biochim. Biophys. Acta-Gen. Subj*. 2002, 1573, 177-182.

14. Yin, C.; Zhou, F. Y.; Wang , Y. R.; Luo, W. H.; Luo, Q. M. ; Li, P. C. Simultaneous detection of hemodynamics, mitochondrial metabolism and light scattering changes during cortical spreading depression in rats based on multi-spectral optical imaging. *Neuroimage.* 2013**,** 76, 70-80.

15. Birkmayer G. D.; Kay, G. G.; Vürre E.; Stabilized NADH (ENADA) improves jet lag-induced cognitive performance deficit. *Wien Med Wochenschr*. 2002, 152, 450-454.

16. Kuila, T.; Bose, S.; Khanra, P.; Mishra, A. K.; Kim, N. H. Recent advances in graphene-based biosensors *Biosens. Bioelectron*. 2011, 26, 4637-4648.

17. Shao, Y.; Wang, J.; Wu, H.; Liu, J.; Aksay, I. A.; Lin, Y. H. Graphene Based Electrochemical Sensors and Biosensors: A Review. *Electroanalysis.* 2010**,** 22, 1027-1036.

18. Radoi, A.; Compagnone, D. Recent advances in NADH electrochemical sensing design. *Bioelectrochemistry.* **2009**, 76, 126-134.

19. Basova, T.; Gurek A.G.; Ahsen V.; Ray, A. K. Electrochromic lutetium phthalocyanine films for in situ detection of NADH. *Opt. Mater.* **2013**, 35, 634-637.

20. Basova T.; Jushina I.; Guerek A.G.; Ahsen V.; Ray A.K. Use of the electrochromic behaviour of lanthanide phthalocyanine films for nicotinamide adenine dinucleotide detection. *J. R. Soc. Interface*. 2008, 5, 801-806.

21. Pal C, Cammidge AN, Cook MJ, Sosa-Sanchez JL, Sharma AK, Ray, AK. In situ chemichromic studies of interactions between a lutetium bis-octaalkyl-substituted phthalocyanine and selected biological cofactors. *J. R. Soc. Interface* **2012**, 9, 183-189

22. Chaure, N. B.; Sosa-Sanchez, J. L.; Cammidge, A. N.; Cook, M. J.; Ray, A. K. Solution processable lutetium phthalocyanine organic field-effect transistors. *Org. Electron.* 2010, 11, 434-438.

23. Wang, H. L.; Kobayashi, N.; Jiang, J. Z.; New Sandwich-Type Phthalocyaninato-Metal Quintuple-Decker Complexes. *Chem.-Eur. J*. 2012, 18(4), 1047-1049.

24. Sergeyev, S.; Pouzet, E. Debever, O.; Levin, J.; Gierschner, J.; Cornil, J.; Aspe, R.G. ; Geerts, Y. H. Liquid crystalline octaalkoxycarbonyl phthalocyanines: design, synthesis, electronic structure, self-aggregation and mesomorphism. J. Mater. Chem. 2007, 17(18), 1777-1784

25. Swarts, J. C.; Langner, E. H. G.; Krokeide-Hove, N.; Cook, M. J. Synthesis and electrochemical characterisation of some long chain 1,4,8,11,15,18,22,25-octa-alkylated metal-free and zinc phthalocyanines possessing discotic liquid crystalline properties. *J. Mater. Chem.* 2001, 11(2), 434-443.

26. Kadish, K. M.; Nakanishi, T.; Gurek, A.; Ahsen, V.; Yilmaz, I. Electrochemistry of a double-decker lutetium(III) phthalocyanine in aqueous media. The first evidence for five reductions. J. Phys. Chem. B. 2001 105(40), 9817-9821
27. Neudeck, A.; Marken, F.; Compton, R. G. Complex electron transfer kinetic data from convolution analysis of cyclic voltammograms. Theory and application to diamond electrodes. *Electroanalysis* 1999, 11, 1149-1154.
28. Zhu, P. H.; Lu, F.L.; Pan, N.; Arnold, D. P.; Zhang, S. Y.; Jiang, J. Z. Comparative electrochemical study of unsubstituted and substituted bis(phthalocyaninato) rare earth(III) complexes *Eur. J. Inorg. Chem.* 2004, 3, 510-517.
29. Quentel, F. l.; Elleouet, C.; Mirceski, V.; Hernandez, V. A.; L'Her, M.; Lovric, M.; Komorsky-Lovric, S.; Scholz, F. *J.* Studying ion transfers across a room temperature ionic liquid vertical bar aqueous electrolyte interface driven by redox reactions of lutetium bis(tetra-tert-butylphthalocyaninato) *Electroanal. Chem.* 2007**,** 611, 192-200.
30. Martin, M. G.; de Saja, J. A.; Munoz, R.; Rodriguez-Mendez, M. L. Multisensor system based on bisphthalocyanine nanowires for the detection of antioxidants. *Electrochim. Acta.* 2012, 68, 88-94.
31. Nakanishi, T.; Yilmaz, I.; Nakashima, N.; Kadish, K. M. Thermodynamic Study of Ion-Pairing Effects Between Reduced Double-Decker Lutetium(III) Phthalocyanines and A Cationic Matrix. *J. Phys. Chem. B* 2003, 107, 12789-12796.
32. Li, X. F.; Zhang, S. X.; Sun, C. Q. Fabrication of a covalently attached multilayer film electrode containing cobalt phthalocyanine and its electrocatalytic oxidation of hydrazine. *J. Electroanal. Chem.* 2003, 553, 139-145
33. Orti, E.; Bredas J. L.; Clarisse, C. Electronic-Structure of Phthalocyanines - Theoretical Investigation of the Optical-Properties of Phthalocyanine Monomers, Dimers, And Crystals *J. Chem. Phys.* 1990, 92, 1228-1235
34. Rousseau, R.; Aroca, R.; Rodriguezmendez, M. L. Extended Huckel Molecular-Orbital Model for Lanthanide Bisphthalocyanine Complexes *J. Mol. Struct.* **1995**, 356, 49-62.
35. Bao, M.; Wang, R. M.; Rintoul, L.; Liu, Q. Y.; Arnold, D. P.; Ma, C. Q.; Jiang, J.Z. Vibrational Spectroscopy of Phthalocyanine and Naphthalocyanine in Sandwich-Type (Na)Phthalocyaninato and Porphyrinato Rare Earth Complexes - Part 12 - Part 13. The Raman Characteristics of Phthalocyanine in Unsubstituted And Peripherally Octa(Octyloxy) -Substituted Homoleptic Bis(Phthalocyaninato) Rare Earth Complexes. *Polyhedron* 2006, 25, 1195-1203.

36. Vivas, M.G.; Fernandes, E. G. R.; Rodriguez-Mendez, M. L. Mendonca, C.R. Study of Singlet Excited State Absorption Spectrum of Lutetium Bisphthalocyanine using the Femtosecond Z-Scan Technique. *Chem. Phys. Lett*., 2012, 531, 173-176.

37. Takamatsu, S.; Ishikawa, N. A Theoretical Study of a Drastic Structural Change of Bis(Phthalocyaninato)Lanthanide by Ligand Oxidation: Towards Control of Ligand Field Strength and Magnetism of Single-Lanthanide-Ionic Single Molecule Magnet. *Polyhedron.* 2007, 26, 1859-1862.

38. Koca, A.; Ceyhan, T.; Erbil, M. K.; Ozkaya, A.R.; Bekaroglu, O. Electrochemistry and Spectroelectrochemistry of Tert-Butylcalix[4]Arene Bridged Bis Double-Decker Lutetium(111) Phthalocyanine, Lu_2Pc_4 and Dimeric Lutetium(III) Phthalocyanine, $Lu_2Pc_2(Oac)(2)$. *Chem. Phys.* 2007**,** 340, 283-292.

39. Deore, B. A.; Freund, M. S. Reactivity of poly(anilineboronic acid) with NAD(+) and NADH. *Chem. Mater.* 2005, 17, 2918–2923.

40. Bao, M.; Wang, R. M.; Rintoul, L.; Arnold, D. P.; Jiang, J. Z. Vibrational spectroscopy of phthalocyanine and naphthalocyanine in sandwich-type (na)phthalocyaninato and porphyrinato rare earth complexes - Part 14. The infrared and Raman characteristics of phthalocyanine in "pinwheel-like" homoleptic bis[1,8,15,22-tetrakis(3-pentyloxy)phthalocyaninato] rare earth(III) double-decker complexes *Vib. Spectrosc.* 2006, 40 47-54.

41. Tran-Thi, T.H.; Mattioli, T. A.; Chabach, D.; de Cian, A.; Weiss, R. Hole Localization or Delocalization - An Optical, Raman, And Redox Study of Lanthanide Porphyrin-Phthalocyanine Sandwich-Type Heterocomplexes. *J. Phys. Chem*. 1994, 98, 8279–8288.

42. Jiang, J.Z.; Bao, M.; Rintoul, L.; Arnold, D. P. Vibrational spectroscopy of phthalocyanine and naphthalocyanine in sandwich-type (na)phthalocyaninato and porphyrinato rare earth complexes *Coord. Chem. Rev.* 2006, 250, 424-448.

43. Jiang J.Z.; Rintoul, L.; Arnold D. P. Raman spectroscopic characteristics of phthalocyanine and naphthalocyanine in sandwich-type (na)phthalocyaninato and porphyrinato rare earth complexes. *Polyhedron*. 2000**,** 19, 1381-1394

Figure captions

Figure1: (a) Bis[1,4,8,11,15,18,22,25-octakis(octyl)phthalocyaninato] lutetium(III) [$R_{16}LuPc_2$ R = C_8H_{17} (octyl) chains], (b) Cyclic voltammogram of 0.33 M $R_{16}LuPc_2$ in DCM solvent with 0.1 M TBAP at 25 °C. Scan rate 100mV/sec. (c) Cyclic voltammogram of $R_{16}LuPc_2$ spun film on ITO electrode in a 1.5 M LiClO4 aqueous solution at 25 °C. Scan rate 100mV/sec. Inset, dependence of the anodic peak current obtained in an aqueous solution of 1.5 M $LiClO_4$ (solid squares) and 1 M KCl (open squares) on number of cycles and (d) Current density time transients at applied oxidising potential 0.88 V for 20 minutes in 1.5 M $LiClO_4$. (Inset) logarithmic plots of Current density vs time at same applied potential.

Figure 3: Electronic absorption spectra of $R_{16}LuPc_2$ as (a) fresh solution in chloroform (solid line), (b) neutral film (broken line), (c) Br_2-oxidized film (dotted line) and (d) electrochemically oxidized film (dotted line), Inset shows the optical transition between molecular orbitals.

Figure 4: Electronic absorption spectra of three month old R_{16} $LuPc_2$: (a) neutral solution (solid line) (a) neutral film (broken line) and (b) Br_2-oxidized film (dotted line).

Figure 5: The change of optical absorption spectra of 3 month old $R_{16}LuPc_2^+$ film in 0.5mM NADH dissolved in 1.5 M $LiClO_4$ with time (a) 4 mins, (b) 17 mins, (c) 38 mins and (d) 90 mins. Insets show (A) the plot of decrease in intensity of the Q-band against time of reduction on logarithm-linear scale and dependence of oxidation half-life on NADH concentration for freshly prepared (solid line) and 3months old (dotted) films.

Figure 6: Raman spectra drop cast films on glass substrates: (a) neutral, (b) Br_2-oxidised, (c) partially reduced by NADH reaction and (d) completely reduced by NADH reaction (during the course of reaction. The excitation wavelength was equal to 632.8 nm in each case.

Figure 7: (a) Raman spectra of 3 months old drop cast film (A) neutral and (B) oxidised. (b) Histograms in Inset showing relative intensities at two peaks occurring in the range of (A) 748cm^{-1} -780cm^{-1} (B) 1335 cm^{-1} - 1406 cm^{-1}.

Table1: Wavenumber locations of characteristic Raman bands of neutral and oxidised $R_{16}LuPc_2$.

Position of Raman peak for R_{16} $LuPc_2$ films in		Assignment	References
Neutral state (cm^{-1})	Oxidised state (cm^{-1})		
297 (296)	297 (299)	Lu-N, isoindole bending	
631 (631)	639 (633)	Pc ring breathing	[43]
688 (689)	683	Pc ring breathing	[37],[43]
748 (749)	751 (749)	Aromatic C-H wag	[37],[43]
777 (775)	780 (778)	C=N aza stretching	[37]
942 (932)	942 ----	Benzene ring bending	[37]
1078 (1076)	1081 (1087)	Aromatic C-H bending	[43]
----	1204 (1203)	Aromatic C-H bending	[43]
1227 (1231)	1237 (1240)	Aromatic C-H bending	[20]
1335 (1341)	1352 (1348)	Pyrrole C=C stretching	[43]
1402 (1397)	1406 (1405)	Isoindole stretching	[37]
1510 (1511)	1519 (1519)	Coupling of C=C pyrrole and aza C=N stretching	[37],[43]
1603 (1592)	1609 (1608)	Benzene stretching	[37]

Values in parenthesis are the peak positions for 3 months old film.

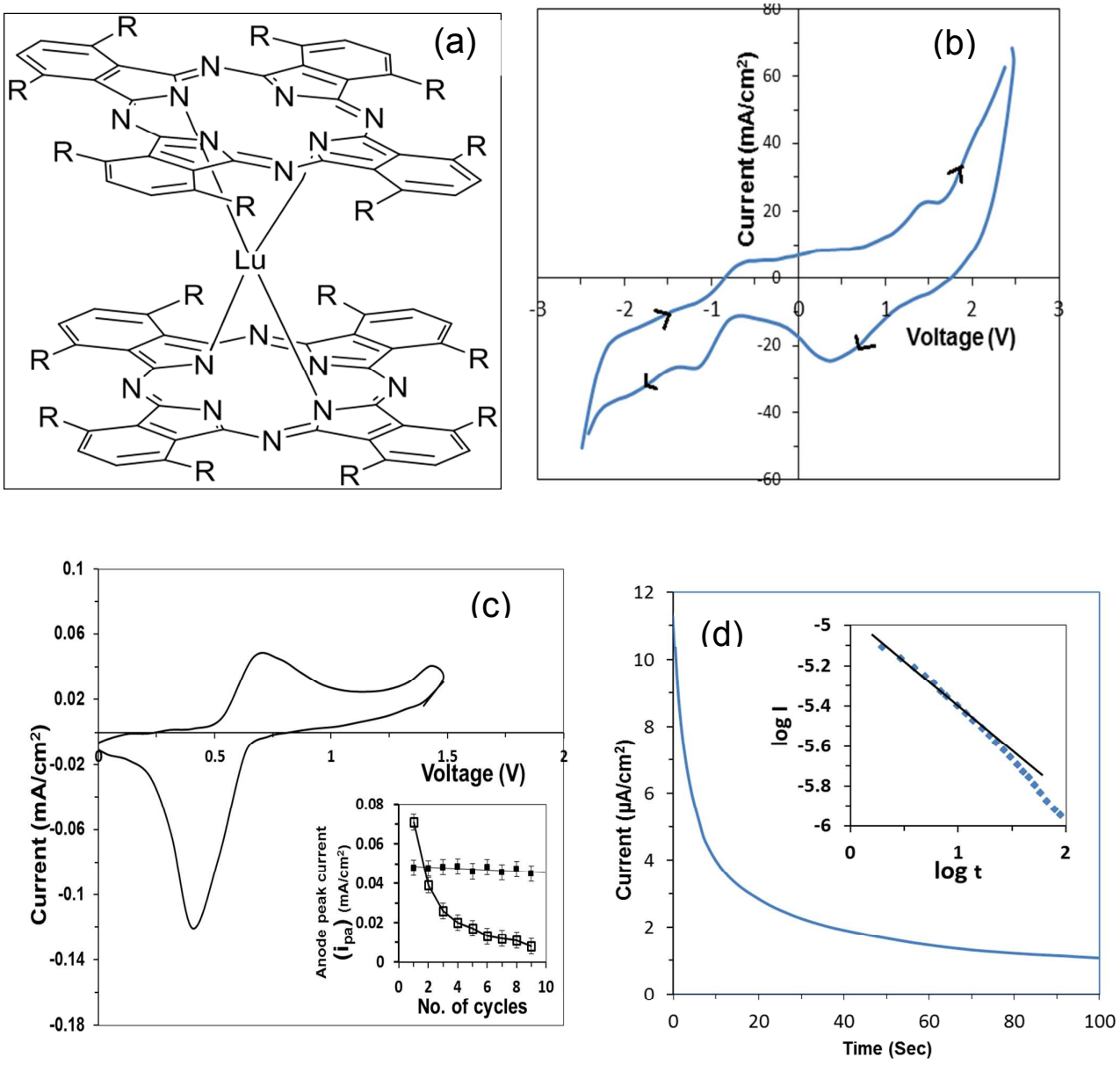

Figure1: (a) Bis[1,4,8,11,15,18,22,25-octakis(octyl)phthalocyaninato] lutetium(III) [$R_{16}LuPc_2$ R = C_8H_{17} (octyl) chains], (b) Cyclic voltammogram of 0.33 M $R_{16}LuPc_2$ in DCM solvent with 0.1 M TBAP at 25 °C. Scan rate 100mV/sec. (c) Cyclic voltammogram of $R_{16}LuPc_2$ spun film on ITO electrode in a 1.5 M LiClO4 aqueous solution at 25 °C. Scan rate 100mV/sec. Inset, dependence of the anodic peak current obtained in an aqueous solution of 1.5 M $LiClO_4$ (solid squares) and 1 M KCl (open squares) on number of cycles and (d) Current density time transients at applied oxidising potential 0.88 V for 20 minutes in 1.5 M $LiClO_4$. (Inset) (Inset) logarithmic plots of Current density vs time at same applied potential.

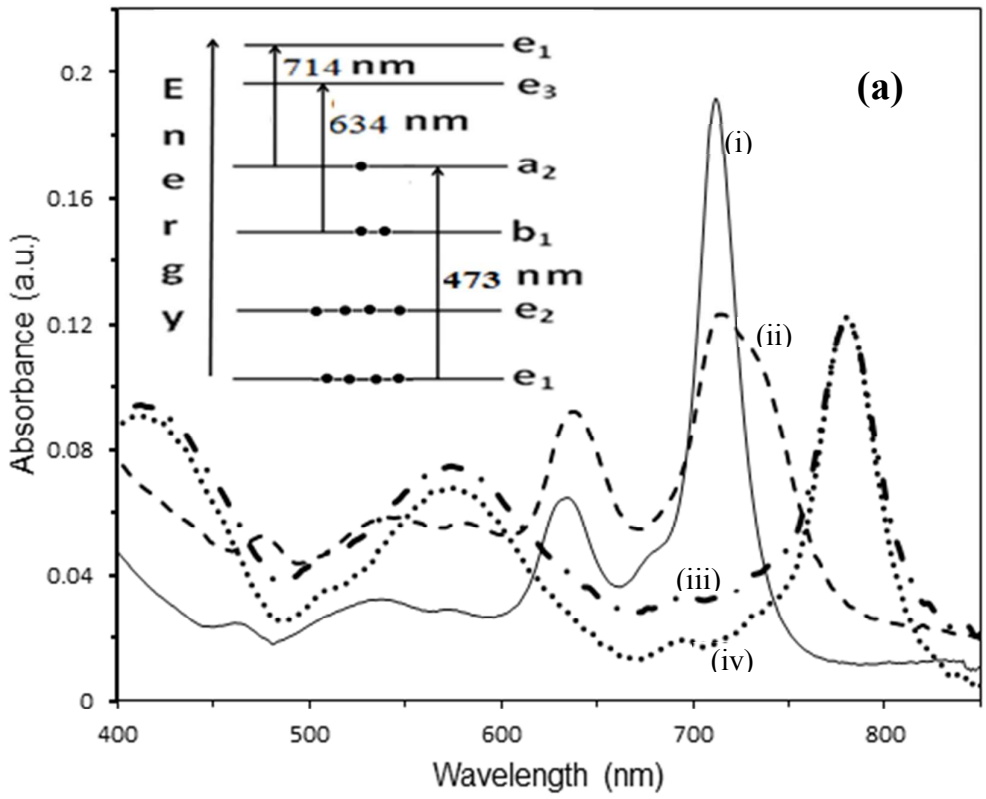

Figure 3: Electronic absorption spectra of $R_{16}LuPc_2$ as (a) fresh solution in chloroform (solid line), (b) neutral film (broken line), (c) Br_2-oxidized film (dotted line) and (d) electrochemically oxidized film (dotted line), Inset shows the optical transition between molecular orbitals.

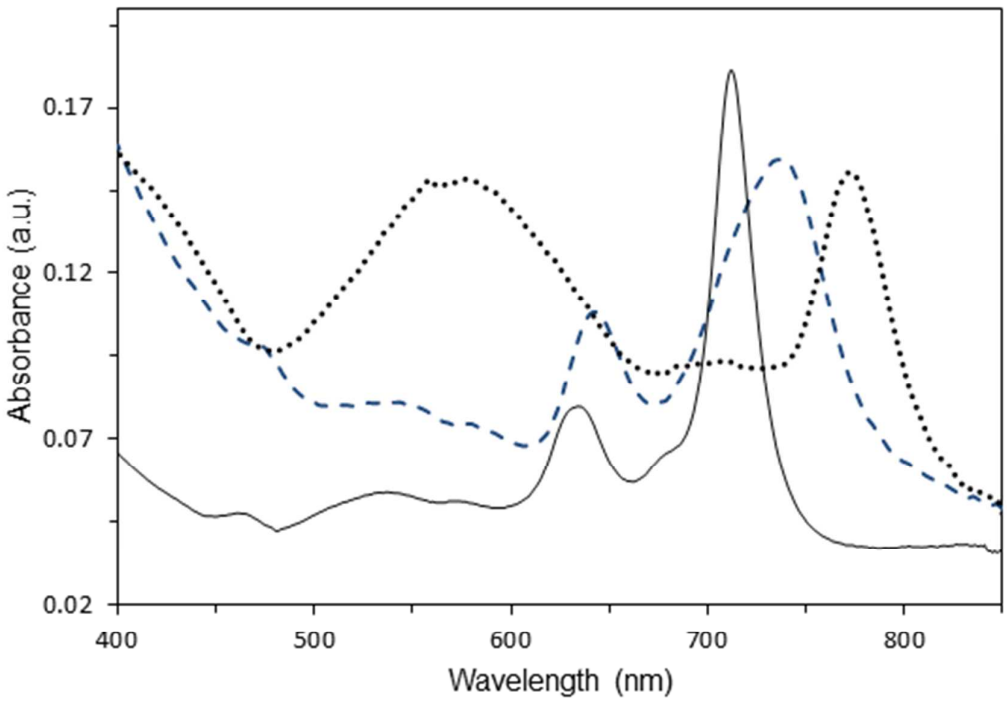

Figure 4: Electronic absorption spectra of three month old R_{16} $LuPc_2$: (a) neutral solution (solid line) (a) neutral film (broken line) and (b) Br_2-oxidized film (dotted line).

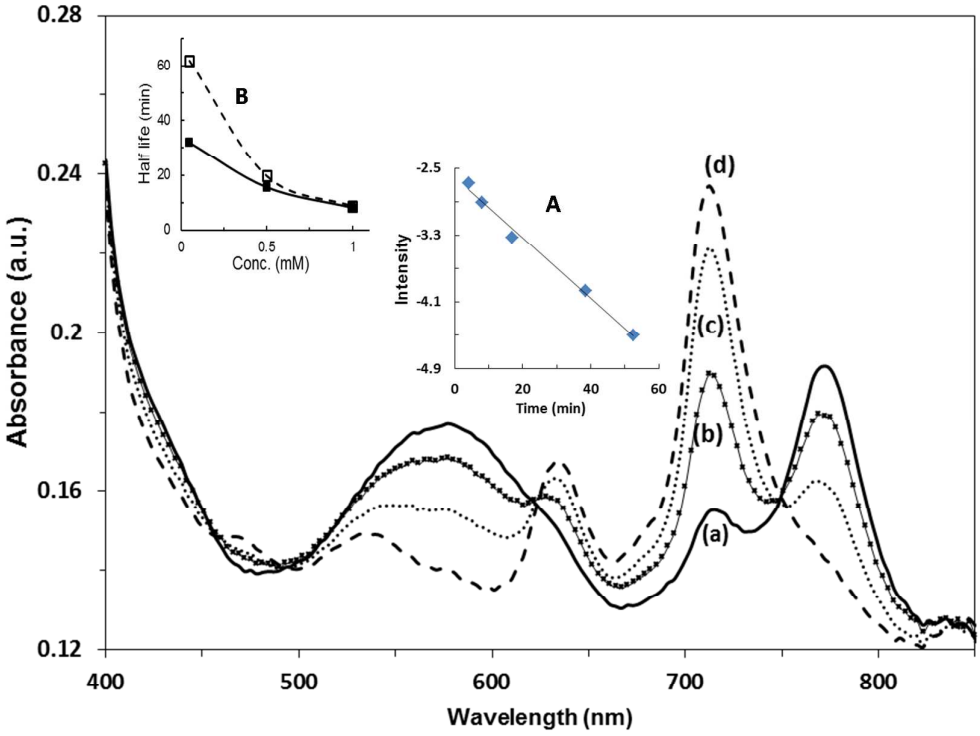

Figure 5: The change of optical absorption spectra of 3 month old $R_{16}LuPc_2^+$ film in 0.5mM NADH dissolved in 1.5 M $LiClO_4$ with time (a) 4 mins, (b) 17 mins, (c) 38 mins and (d) 90 mins. Insets show (A) the plot of decrease in intensity of the Q-band against time of reduction on logarithm-linear scale and dependence of oxidation half-life on NADH concentration for freshly prepared (solid line) and 3months old (dotted) films.

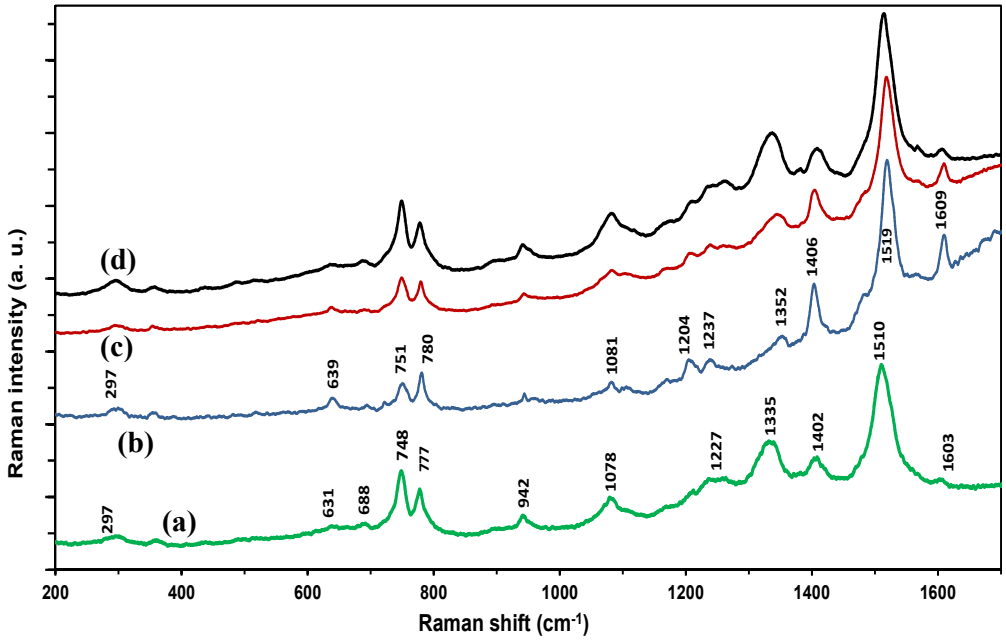

Figure 6: Raman spectra drop cast films on glass substrates: (a) neutral, (b) Br_2-oxidised, (c) partially reduced by NADH reaction and (d) completely reduced by NADH reaction (during the course of reaction. The excitation wavelength was equal to 632.8 nm in each case.

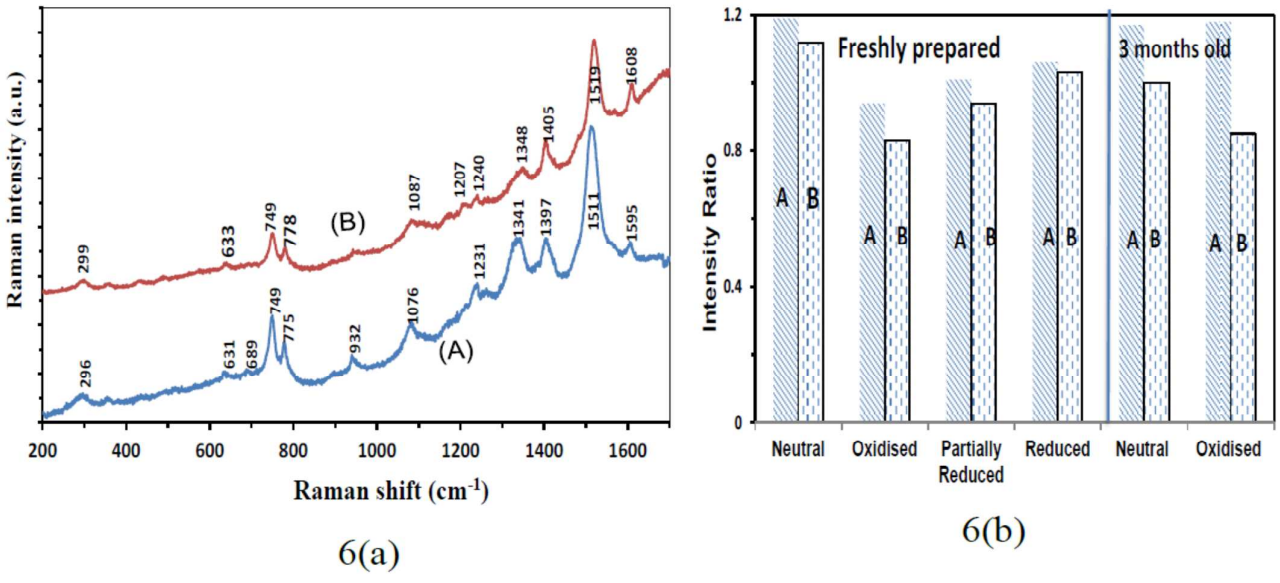

Figure 7: (a) Raman spectra of 3 months old drop cast film (A) neutral and (B) oxidised. (b) Histograms in Inset showing relative intensities at two peaks occurring in the range of (A) 748cm^{-1} -780cm^{-1} (B) 1335 cm^{-1} - 1406 cm^{-1}.

.

A graphic

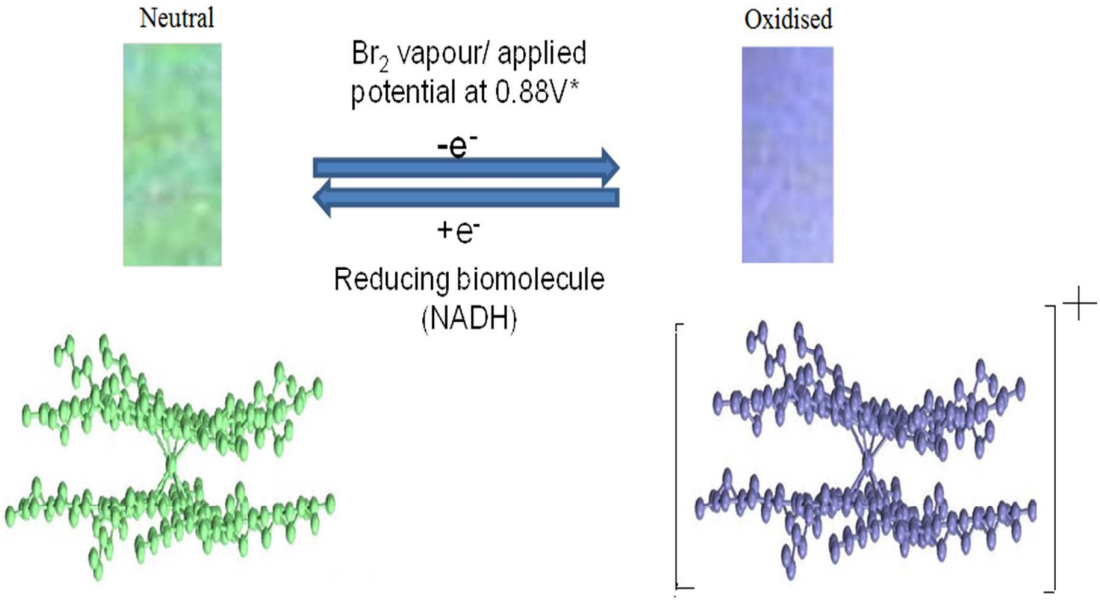
Neutral
Br2 vapour/ applied potential at 0.88V*
-e-
+e-
Reducing biomolecule (NADH)
Oxidised